MODIFICATION OF k-ω TURBULENCE MODEL FOR SHIP FLOW PREDICTION

Takanori Hino[1,*], Kengo Suzuki[1] and Youhei Takagi[1]

[1] Yokohama National University
Yokohama, Kanagawa, 240-8501 Japan.
E-mail: hino-takanori-nf@ynu.ac.jp, web page: http://www.ynu.ac.jp/

[*] Corresponding author: Takanori Hino, hino-talanori-nf@ynu.ac.jp

ABSTRACT

CFD analysis has become an essential tool in ship hydrodynamics both for practical design applications and for engineering researches. However, although the many efforts are being devoted to the development of turbulence modeling, universal turbulence models which can be applied to a wide class of flows are not yet established. Particularly, ship flows are characterized as turbulent flows with separation around complex geometry and this makes the modeling even more difficult. In the current ship flow simulations, the turbulence model must be carefully selected from the experiences and the optimal model varies case by case. Recently, a new concept is proposed for expanding flexibility and applicability of the RANS turbulence model. This approach called GEKO (GEneralized K-Omega) (Menter et al., 2019) makes modification to the existing SST model (Menter, 1994) by adding free parameters to control the various properties such as separation, curvature correction, near wall treatment and so on. Inspired by this approach, the parameter tuning of the SST model is attempted in the present study to improve the prediction capability of the k-ω turbulence model for ship flow applications.

Keywords: CFD; Ship Flow; Resistance; Boundary Layer; Wake; Turbulence Model.

NOMENCLATURE

B_{WL}	Breadth on waterline of a ship
C_B	Block coefficient of a ship
C_s	Turbulence model parameter for flow separation control
C_{RC}	Turbulence model parameter for rotation/curvature correction
k	Turbulent kinetic energy
L_{PP}	Length between perpendiculars of a ship
Re	Reynolds number ($=UL_{PP}/\nu$)
U	Uniform Velocity
ν	Kinematic viscosity of water
ρ	Water density
ω	Specific turbulent dissipation rate

1 INTRODUCTION

CFD analysis has become an essential tool in ship hydrodynamics both for practical design applications and for engineering researches. Furthermore, ship CFD applications are extended to more complex problems such as seakeeping and maneuvering and to more detailed geometry with propulsors, rudder and energy saving devices. From a physics-based point of view, however, the present CFD predictions have severe limitation coming from turbulence modeling. Although the many efforts are being devoted to the development of turbulence modeling, universal turbulence models which can be applied to a wide class of flows are not yet established. Particularly, ship flows are characterized as turbulent flows

with separation around complex geometry and this makes the modeling even more difficult. In the current ship flow simulations, the turbulence model must be carefully selected from the experiences and the optimal model varies case by case. The turbulence models suitable for resistance predictions are not necessarily optimal for wake reproduction and vice versa. Though Large Eddy Simulation (LES) is expected to be one of the possible solutions, excessive computing resources required for LES is still prohibitive for practical applications. Therefore, RANS (Reynolds Averaging Navier-Stokes) models are considered to be a workhorse at least for a while.

Recently, the new concept is proposed to expand flexibility and applicability of the RANS turbulence model. This approach called GEKO (GEneralized K-Omega) (Menter et al., 2019) makes modification to the existing SST model (Menter, 1994) by adding free parameters to control the various properties such as separation, curvature correction, near wall treatment and so on. Unfortunately, the detail of the implementation of GEKO is not disclosed.

Inspired by this approach, the parameter tuning of the SST model is attempted in the present study to improve the prediction capability of the k-ω turbulence model for ship flow applications. New parameters are introduced for the separation behavior and the rotation correction both of which are relevant to ship stern flows. Flow fields with different parameter values for a benchmark ship hull are examined and the proper parameter set are explored to achieve better predictions of both resistance estimation and velocity distributions at multiple stations.

2 TURBULENCE MODELING

2.1 k-ω SST Model

The turbulence model modification is based on the k-ω SST model (Menter, 1994). The original model is the hybrid model combining the k-ω model and k-ϵ model. The basic equations for k (turbulent kinetic energy) and ω (specific turbulent dissipation rate) are expressed in the non-dimensional form as

$$\frac{Dk}{Dt} = T_{ij}\frac{\partial u_i}{\partial x_j} - \beta^*\omega k + \frac{\partial}{\partial x_j}\left\{\left(\frac{1}{Re} + \sigma_k\nu_t\right)\frac{\partial k}{\partial x_j}\right\} \tag{1}$$

$$\frac{D\omega}{Dt} = \frac{\gamma}{\nu_t}T_{ij}\frac{\partial u_i}{\partial x_j} - \beta\omega^2 + \frac{\partial}{\partial x_j}\left\{\left(\frac{1}{Re} + \sigma_\omega\nu_t\right)\frac{\partial \omega}{\partial x_j}\right\} + 2(1-F_1)\sigma_{\omega 2}\frac{1}{\omega}\frac{\partial k}{\partial x_j}\frac{\partial \omega}{\partial x_j} \tag{2}$$

where T_{ij} is the turbulent shear stress tensor

$$T_{ij} = \nu_t(\frac{\partial u_i}{\partial x_j} + \frac{\partial u_j}{\partial x_i}) - \frac{2}{3}k\delta_{ij}.$$

F_1 is the blending function defined as

$$F_1 = \tanh(arg_1^4)$$

with

$$arg_1 = \min\left(\max\left(\frac{\sqrt{k}}{0.09\omega d}, \frac{500/Re}{d^2\omega}\right), \frac{4\sigma_{\omega 2}k}{CD_{k\omega}d^2}\right)$$

where d is the distance to the closest wall. $CD_{k\omega}$ is defined as

$$CD_{k\omega} = \max\left(2\sigma_{\omega 2}\frac{1}{\omega}\frac{\partial k}{\partial x_j}\frac{\partial \omega}{\partial x_j}, 10^{-20}\right).$$

The eddy viscosity ν_t is evaluated as

$$\nu_t = \frac{a_1 k}{\max(a_1\omega, \Omega F_2)}$$

where Ω is the magnitude of the vorticity and $a_1 = 0.31$. F_2 is the function defined as

$$F_2 = \tanh(arg_2^2), \quad arg_2 = \max\left(2\frac{\sqrt{k}}{0.09\omega d}, \frac{500/Re}{d^2\omega}\right)$$

where Re is the Reynolds number. The constants appeared above are blended using F_1 as

$$\phi = F_1\phi_1 + (1 - F_1)\phi_2$$

where ϕ is σ_k, σ_ω, β or γ. The subscripts 1 and 2 correspond to the inner (k-ω) and outer (k-ϵ) constants, respectively. The constants in the inner region are :

$$\sigma_{k1} = 0.85, \quad \sigma_{\omega 1} = 0.5, \quad \beta_1 = 0.0750, \quad \beta^* = 0.09$$

and

$$\gamma_1 = \frac{\beta_1}{\beta^*} - \frac{\sigma_{\omega 1}\kappa^2}{\sqrt{\beta^*}}$$

with $\kappa = 0.41$. While the constants in the outer region are:

$$\sigma_{k2} = 1.0, \quad \sigma_{\omega 2} = 0.856, \quad \beta_2 = 0.0828, \quad \beta^* = 0.09$$

and

$$\gamma_2 = \frac{\beta_2}{\beta^*} - \frac{\sigma_{\omega 2}\kappa^2}{\sqrt{\beta^*}}.$$

2.2 Separation Parameter

The parameter C_s is introduced for the control of the boundary layer separation behavior. With the parameter C_s, the inner constants ϕ_1 (σ_{k1}, $\sigma_{\omega 1}$ or β_1) are modified as

$$\phi_1' = \phi_2 + (\phi_1 - \phi_2)\frac{C_s - 1.0}{0.75}$$

Thus, $C_s = 1.75$ yields $\phi_1' = \phi_1$ and the model is equivalent to the original SST model. $C_s = 1.0$ corresponds to $\phi_1' = \phi_2$ and the model is equivalent to the k-ϵ model since the constants are equal to the outer (k-ϵ) values everywhere. Since the $k - \omega$ model is considered to give more pronounced flow separation than the $k - \epsilon$ model, the increase of C_s can enhance the separation intensity of a flow field.

2.3 Rotation/Curvature Correction

The rotation/curvature correction of Hellsten (Hellsten, 1998) is known to be effective to reproduce the longitudinal vortices of a ship wake. In the correction, the destruction term $\beta\omega^2$ of the ω equation (2) is replaced with $F_4\beta\omega^2$, where

$$F_4 = \frac{1}{1 + C_{RC}R_i}$$

$$R_i = \frac{W}{S}\left(\frac{W}{S} - 1\right)$$

$$S = \sqrt{2S_{ij}S_{ij}}, \quad S_{ij} = \frac{1}{2}\left(\frac{\partial u_i}{\partial x_j} + \frac{\partial u_j}{\partial x_i}\right)$$

$$W = \sqrt{2W_{ij}W_{ij}}, \quad W_{ij} = \frac{1}{2}\left(\frac{\partial u_i}{\partial x_j} - \frac{\partial u_j}{\partial x_i}\right)$$

The parameter C_{RC} is used to define the amount of correction.

2.4 Spatial Distributions of Parameters

In the previous study(Hino et al., 2020), the parameters C_s and C_{RC} are assumed to have the same values in the whole domain. In order to increase flexibility of the model, the extension is made to enable the spatial distributions of parameters. The parameter C_* where $*$ is ether s or RC is defined as

$$C_* = \begin{cases} C_{*,1} & \text{if } x \leq x_{*,1} \\ C_{*,1} + (C_{*,2} - C_{*,1})\frac{x - x_{*,1}}{x_{*,2} - x_{*,1}} & \text{if } x_{*,1} \leq x \leq x_{*,2} \\ C_{*,2} & \text{if } x_{*,2} \leq x \end{cases} \tag{3}$$

where x is the coordinate in the flow direction with its origin at FP. Thus, each parameter C_* has the values between $C_{*,1}$ and $C_{*,2}$ depending on the x coordinate.

2.5 Implementation

The model is implemented in the incompressible unstructured Navier-Stokes solver *SURF* ver. 7 (Hino, 1997). The solver is based on the 2nd order finite-volume discretization with artificial compressibility for velocity-pressure coupling. The spatial discretizations of the flow equations are the second order upwind scheme for the inviscid terms and the central scheme for the viscous terms except that the convection terms on the turbulence equations for which the first order upwind scheme is adopted. Time integration is carried out using the Euler implicit scheme for the present steady-state simulation.

3 RESULTS AND DISCUSSION

3.1 Ship Model

A ship model used is JBC (Japan Bulk Carrier) (Hino et al., 2016) which is a relatively new benchmark hull of a bulk carrier with an energy saving duct. It was used as one of the test cases in the CFD Workshop Tokyo 2015 (Hino et al., 2021). The bare hull configuration without a rudder is considered in the present study. The particulars of JBC in ship and model scales are listed in Table 1. Model scale simulation is performed where free surface effects are neglected for simplicity.

Table 1. Principal Particulars of Japan Buck Carrier (JBC)

	Ship	Model
L_{PP} (m)	280.0	7.00
L_{WL} (m)	285.0	7.125
B_{WL} (m)	45.0	1.125
T (m)	16.5	0.4125
C_B	0.8580	

3.2 Grid and Conditions

A computational grid for JBC hull is generated with O-O topology using the commercial software Pointwise as shown in Fig. 1. Total number of cells are approximately 1.4 million and the minimum spacing on the wall is set to be $y^+ \approx 1$, since the no-slip boundary condition without a wall function is applied on a wall. Reynolds number is set to 7.46×10^6 and this corresponds to the flow measurement at the towing tank(Hino et al., 2021)

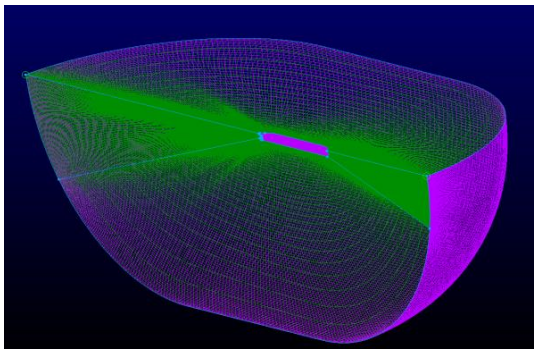

Figure 1. Computational Grid for JBC hull.

3.3 Wake Distributions and Resistance

3.3.1 Case 0

In the previous study(Hino et al., 2020) where the parameters C_s and C_{RC} are assumed to have the constant values in a whole domain, the values $C_s = 1.60$ and $C_{RC} = 4.5$ are found to provide the good prediction both for the wake at the propeller plane and the resistance. This set is identified as Case 0. In Figure 2, the distributions of the axial velocity u/U at the propeller plane ($x/L_{PP} = 0.9843$) are compared between the original SST model and the modified model (Case 0) together with the SPIV (Stereoscopic Particle Image Velocitmetry) data measured at the National Maritime Research Institute(Hino et al., 2021). The wake distribution of Case 0 appears better than the original SST model with respect to the intensity of the so-called 'hook' shape. The resistance of the original model is -3.86% of the tank test data which is estimated as the form factor $1+K$ using ITTC 1957 correlation line. On the other hand, Case 0 setting provides -0.28% of the measure data which is closer than the SST result.

Figure 2. Axial velocity distribution of the original SST model (left) and the modified model(Case 0) (right) at $x/L_{PP} = 0.9843$.

Although the velocity distribution at the propeller plane looks reasonable, the comparisons in the other stations reveal the limitation of the constant parameter approach. Figure 3 shows the comparisons of the velocity distributions at three stations, $x/L_{PP} = 0.9625, 0.9843$ and 1.0. In the distribution at $x/L_{PP} = 0.9625$, the 'hook' shape associated with the longitudinal vortices are weaker than the measured data. Also, the distribution at $x/L_{PP} = 1.0$ shows the lower velocity region below the shaft height.

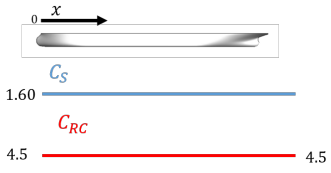

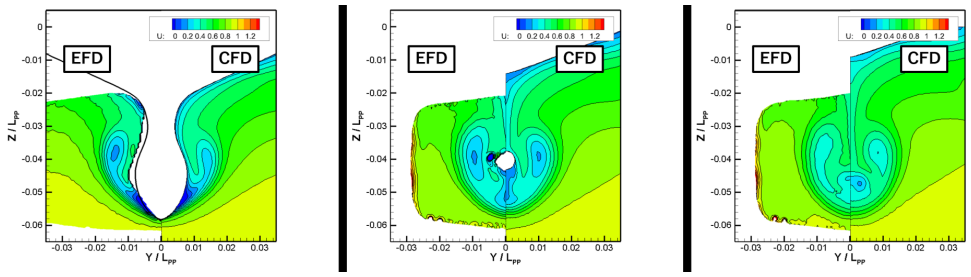

Figure 3. Comparison of axial velocity distributions of the modified $k-\omega$ model (Case 0) at x/L_{PP}=0.9625, 0.9843 and 1.0.

3.3.2 Case 1

Parametric study under the restriction of the constant distribution has been made to obtain the better prediction at the upstream station (x/L_{PP}=0.9625) and it is found that the combination of $C_s = 1.20$ and $C_{RC} = 12.0$ is suitable for the velocity distribution at the upstream. This set is called Case 1. Figure 4 shows the velocity distributions at three stations using Case 1 setting. With the constant parameters, the velocity in the propeller plane and the AP station become worse than case 0 due to the too strong longitudinal vortex. Furthermore, the resistance of this case increases to +5.04% of the measured data.

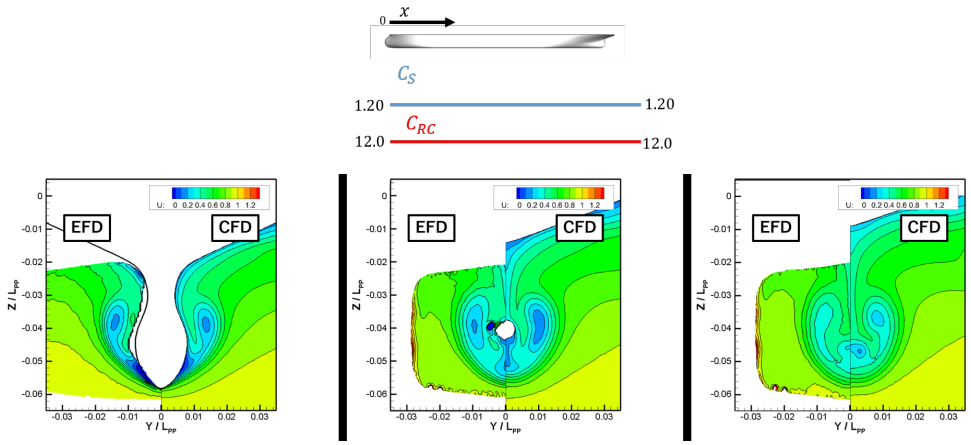

Figure 4. Comparison of axial velocity distributions the modified model (Case 1)at x/L_{PP}=0.9625, 0.9843 and 1.0.

3.3.3 Case 2

In view of the too strong longitudinal vortices in Case 1, the adjustment of the rotation/curvature correction C_{RC} with the varying distribution in x direction is attempted. As the result of some numerical experiments, the following parameter distributions are found to be appropriate with respect to the velocity distributions:

$$C_{RS,1} = 12.0, \quad CRS, 2 = 0.0$$

$$x_{RS,1} = 0.9625, \quad x_{RS,2} = 0.965,$$

with the separation parameter C_s being constant and 1.20. This set is called Case 2 The distributions of the parameters and the velocity distributions are shown in Figure 5. The distributions at three stations reproduce the measured ones reasonably well. Intensity of longitudinal vortices is well consistent with the measured data. However the resistance is still higher, +5.15% of the tank test data.

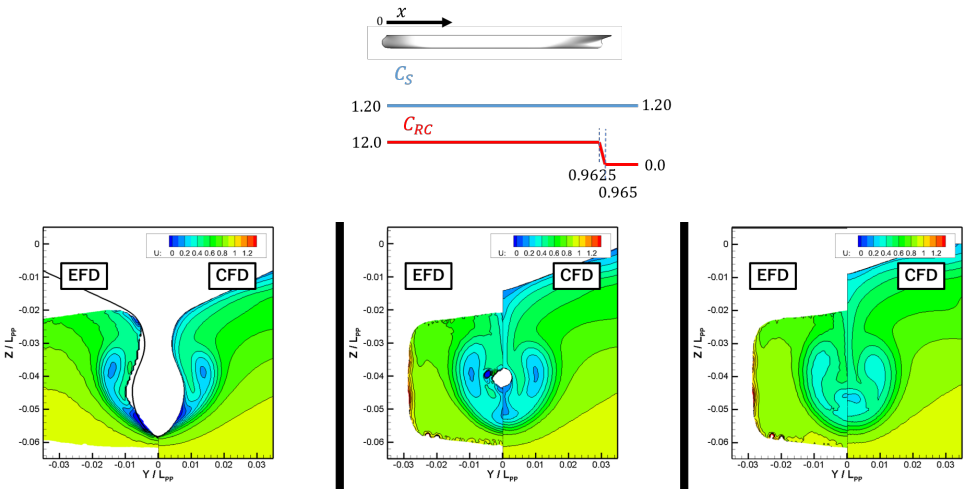

Figure 5. Comparison of axial velocity distributions the modified $k-\omega$ model (Case 2)at x/L_{PP}=0.9625, 0.9843 and 1.0.

3.3.4 Case 3

Although Case 2 provides the reasonable velocity distributions at three stations considered, the resistance is considerably higher than the measured data. The final parameter tuning is performed for the better resistance prediction. From the experience of the previous study(Hino et al., 2020), it is confirmed that the resistance value is sensitive more to the separation parameter C_s while the rotation/curvature parameter C_{RC} hardly affects the resistance value. Therefore, the spatial distribution of C_s is explored and the final parameter setting for C_S is:

$$C_{s,1} = 1.55, \quad Cs, 2 = 1.05$$

$$x_{s,1} = 0.80, \quad x_{s,2} = 0.85,$$

while the setting of C_{RC} is the same as Case 2. This final setting is called Case 3.

In Figure 6, the velocity distributions at three stations are shown together with the parameter distributions. The velocity distributions are almost identical to those of Case 2 and close to the measured distributions and the resistance value is predicted as +0.37% of the tank test data. It is shown that both the velocity distributions at multiple stations and the resistance can be predicted well at the same time with the present parameter setting.

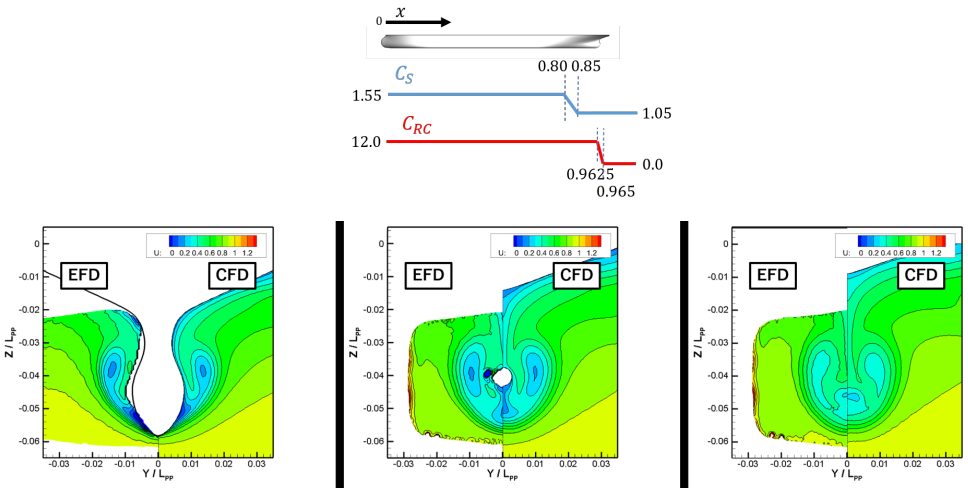

Figure 6. Comparison of axial velocity distributions the modified $k-\omega$ model (Case 3)at x/L_{PP}=0.9625, 0.9843 and 1.0.

3.4 Flow Field Comparisons

In order to examine the flow fields other than the wake distributions at three stations described above, the limiting streamlines and the pressure distributions on a hull surface are compared.

Figure 7 is the comparison of the limiting streamlines on a ship hull surface in the stern region of the original SST model, Case 0 and Case 3. Limiting streamline plots are useful to observe the behaviors of the flow separation patterns. The separation lines of three cases are different from one another particularly the lines running toward the stern tube. Also the direction of the streamlines near the aft-end part is more vertical in the SST model than the other two cases. Since the measured streamlines are not available, it is rather difficult to tell which is the right trend.

Figure 8 shows the hull surface pressure distributions and the axial velocity distributions on a center plane for the original SST model, Case 0 and Case 3. Difference of the surface pressure distribution patterns can be seen at the shaft height between the Case 3 and the other two cases. The low speed region behind the hull is smaller in Case 3 than in Case 0 and the SST.

In the streamlines and the pressure distribution of Case 3, no discontinuity is observed and the smooth flow field is obtained despite the variation of the parameters in x direction.

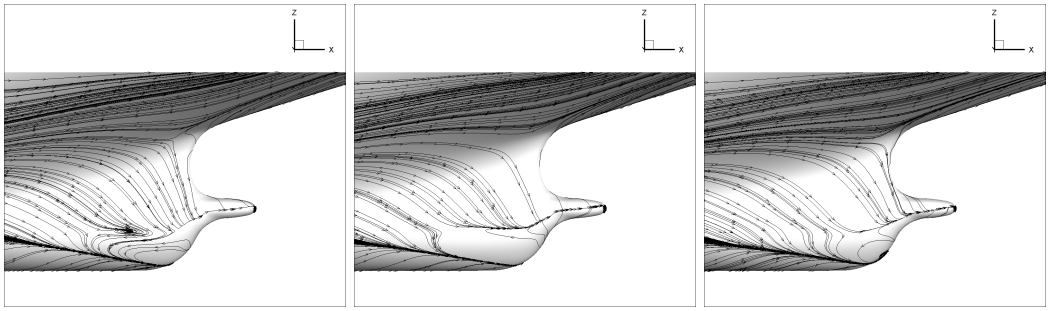

Figure 7. Comparison of limiting streamlines on a ship hull surface: SST (left), Case 0 (middle) and Case 3 (right).

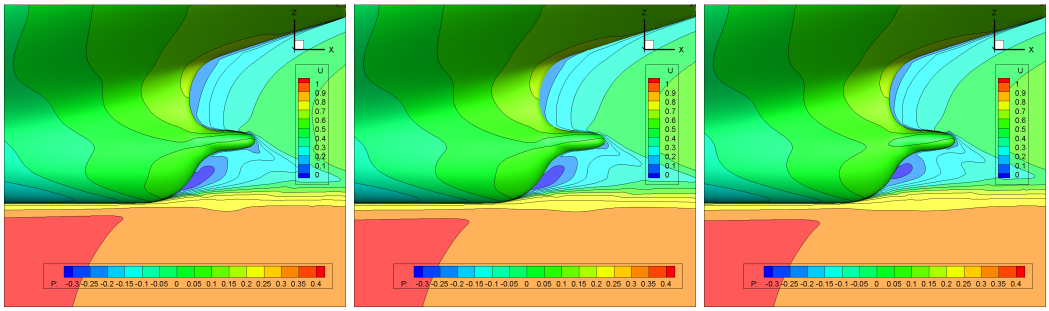

Figure 8. Comparison of pressure distribution of ship hull surface and the axial velocity on a center plane: SST (left), Case 0 (middle) and Case 3 (right).

The distributions of the kinematic turbulent energy k are compared among the original SST, Case 3 and the measured data in Figures 9 to 11 for three stations, x/L_{PP} =0.9625, 0843 and 1.0, respectively. At each station, it is clear that the results of Case 3 show the higher peak values of k compared to the original SST. The higher k values of the present model seem to be closer to the measured data, although the absolute values of the measured data are much higher. Note that the large uncertainty is recognized in the k measurement(Hino et al., 2021).

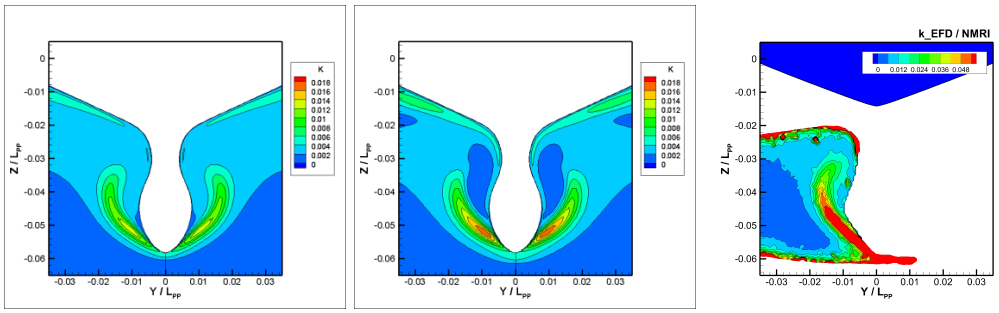

Figure 9. Comparison of turbulent kinetic energy k distributions at $x/L_{PP} = 0.9625$: SST (left), Case 3 (middle), measurement (left)

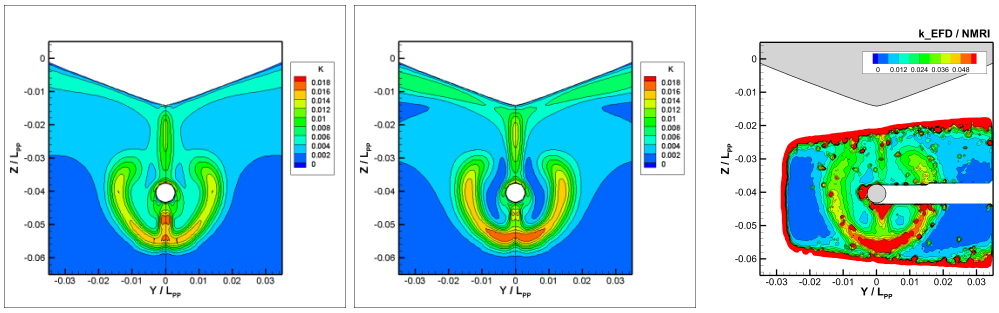

Figure 10. Comparison of turbulent kinetic energy k distributions at $x/L_{PP} = 0.9843$: SST (left), Case 3 (middle), measurement (left)

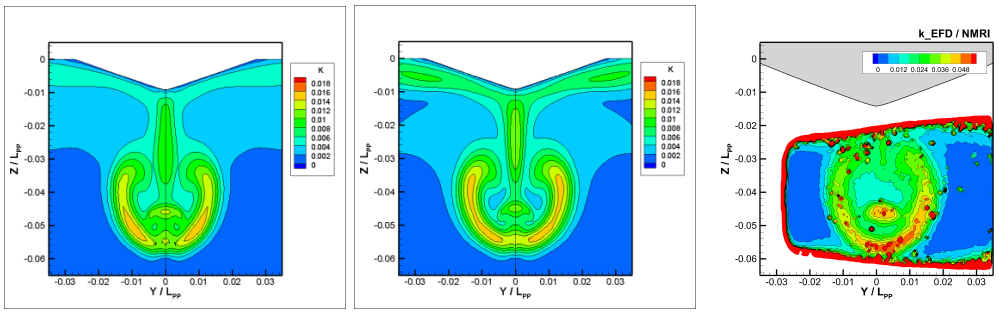

Figure 11. Comparison of turbulent kinetic energy k distributions at $x/L_{PP} = 1.0$: SST (left), Case 3 (middle), measurement (left)

4 CONCLUSIONS

In order to increase the flexibility of the k-ω SST model, the new parameter is introduced which controls the flow separation behavior of the model. Combined with the existing rotation/curvature correction parameter, the parameter tuning to achieve the better prediction of ship stern flows and hull resistance is carried out. The parameter values can be varied in the flow direction using the simple liner distribution functions. In the parametric study, the wake distribution at multiple stations are compared with the measured data and also the predicted resistance is examined against the tank test data. It is shown that the proper choice of the parameter distributions can improve the performance of the turbulence model both in wake distribution and resistance predictions.

In the further investigation, the versatility of the present model will be examined for different classes of ship hulls and finally the way to determine the proper parameter distributions from the ship geometry information needs to be established.

REFERENCES

Hellsten, A. (1998). Some Improvements in Menter's k-omega SST Turbulence Model, *Proc. 29th AIAA Fluid Dynamics Conference*, June 15-18, Albuquerque, USA.

Hino, T. (1997). A 3D Unstructured Grid Method for Incompressible Viscous Flows, *J. of the Society of Naval Architects of Japan*, 182, 9-15.

Hino, T., Hirata, N., Ohashi, K., Toda, Y., Zhu, T., Makino, K., Takai, M., Nishigaki, M., Kimura, K., Anda, M, and Shingo, S. (2016). Hull form design and flow measurements of a bulk carrier with an energy-saving device for CFD validations, *Proc. 13th International Symposium on Practical Design of Ships and other floating structures (PRADS)*, September 4-9, Copenhagen, Denmark.

Hino, T., Suzuki, K., Xu, H. and Takagi, Y. (2020). Parameter Tuning of k-ω Turbulence Model for Ship Flow Simulation, *Conference Proceedings, Japan Society of Naval Architects and Ocean Engineers*, 30, 545-550.

Hino T., Stern F., Larsson L., Visonneau M., Hirata N. and Kim J. (eds) (2021). *Numerical Ship Hydrodynamics. An assessment of the Tokyo 2015 Workshop*, Springer Nature, Switzerland.

Menter, F. R. (1994). Two-equation Eddy-Viscosity Turbulence Models for Engineering Applications, *AIAA Journal*, 32 (8), 1598-1605.

Menter, F. R. and Lechner, R. (2019). Best Practice: Generalized k- Two-Equation Turbulence Model in ANSYS CFD (GEKO), Technical Report ANSYS.